IEEE Access
Multidisciplinary | Rapid Review | Open Access Journal

Received December 28, 2021, accepted January 27, 2022, date of publication January 31, 2022, date of current version February 10, 2022.

Digital Object Identifier 10.1109/ACCESS.2022.3148060

Adaptive Optimal Multi-Surface Back-Stepping Sliding Mode Control Design for the Takagi-Sugeno Fuzzy Model of Uncertain Nonlinear System With External Disturbance

FARZAD SOLTANIAN[1], MOKHTAR SHASADEGHI[1], SALEH MOBAYEN[2,3], (Senior Member, IEEE), AND AFEF FEKIH[4], (Senior Member, IEEE)

[1]Electrical Engineering Faculty, Shiraz University of Technology, Shiraz 715555-313, Iran
[2]Department of Electrical Engineering, University of Zanjan, Zanjan 45371-38791, Iran
[3]Future Technology Research Center, National Yunlin University of Science and Technology, Douliu, Yunlin 64002, Taiwan
[4]Department of Electrical and Computer Engineering, University of Louisiana at Lafayette, Lafayette, LA 70504, USA

Corresponding author: Saleh Mobayen (mobayens@yuntech.edu.tw)

This work was supported in part by the Ministry of Science and Technology (MOST), Taiwan, under Grant MOST 110-2222-E-224-001-.

ABSTRACT This paper proposes a novel scheme of the multi-objective robust control design for a class of uncertain nonlinear systems in strict-feedback-form based on Takagi–Sugeno fuzzy model (TSFM). The nonlinear system contains both the matched and the unmatched uncertainties and also subjected to the external disturbances. The TSFM provides the generalization of the linear systems concepts to the nonlinear systems field in a convex framework. First, a new sliding surface is defined using a convex combination of the surfaces which are defined for each fuzzy rule consequence local linear subsystems. Then, their gains are designed optimally via a generalized eigenvalue problem (GEVP). Also, the upper-bounds of the matched and unmatched uncertainties are estimated using the adaptive update laws. The multi-objective control aims not only to satisfy the H_2-optimization performance, but also, α-stability region is formulated to improve the transient response performance. The H_2-optimization characterization and α-stability design conditions are derived in terms of new linear matrix inequalities (LMIs) conditions. Finally, the effectiveness of the proposed approach is demonstrated by considering a comparative practical example.

INDEX TERMS Back-stepping sliding mode control approaches, H_2-performance, LMI, regional pole placement, Takagi–Sugeno fuzzy model, unknown bounded uncertainty.

I. INTRODUCTION

Takagi-Sugeno (T-S) fuzzy model with sector nonlinearity approaches is commonly used to describe an exact model of a nonlinear system with uncertainties [1]. The basic idea behind the T-S fuzzy approach is to decompose a non-linear system into several local linear models. Then, each linear model aggregates in a convex structure in terms of the normalized weighting. The linear control theory can be applied to each local linear model. After that, the nonlinear control can be obtained by fuzzy blending. These advantages make the T-S fuzzy model a useful tool to model the complex nonlinear system.

The associate editor coordinating the review of this manuscript and approving it for publication was Zheng H. Zhu.

A review of the literature of nonlinear control approaches reveals that the back-stepping mechanism are recognized as a useful method and has been employed in many industrial processes such as drug injection, missiles, AC motors, hybrid electric vehicles, and so on [2]–[8]. In general, it is a systematic and recursive Lyapunov-based design technique through state feedback design that can be employed to the nonlinear systems in a strict feedback form. It can be used to solve both of the stabilization and the tracking control problems [4]. The basic idea of a back-stepping design mechanism is to recursively select appropriate functions of state variables as virtual control inputs for lower dimensions subsystems of the overall system. Thus, the final control outputs can be obtained step by step via selecting a suitable Lyapunov function. Although, backstepping control is a

powerful nonlinear control method [9], [10], but it is not inherently robust against the inevitable undesired phenomena such as uncertainties and external disturbance. To design a robust backstepping control, some robust approaches have been synthesized with this scheme [11], [12]. However, these studies were concerned just for special classes of nonlinear systems including, *e.g.*, strict-feedback systems [13], block-strict-feedback systems [14], [15] and special practical systems [16], [17]. Furthermore, backstepping control does not generate a constrained control input and the previous studies that considered the constrained control are established for a strict class of the systems or special cases [18], [19]. Summary of the above, a universal backstepping control in which incorporate the robustness, constraints and optimality, simultaneously for a wide class of the nonlinear systems is not presented up to now. However, the desired tracking performance for the systems with parameters/ functions uncertainty cannot be guaranteed via back-stepping control law design. The system stability also may be destroyed in some cases. In contrast, sliding mode control (SMC) is a powerful technique that make ensures robustness of the desired system performance in presence of uncertainty [20]–[25]. It has received a great deal of attention in study of nonlinear control field such as biological systems, fault-tolerant control systems, robotic systems, space, and so on [26]–[29]. In addition, SMC has been utilized to compensate the additional uncertainties of the T–S fuzzy system [30]. In [31], for a class of uncertain discrete systems with packet losses, time delays, and ambient noise, a sliding surface was designed. Their studied system can be considered as a linear system with a matched nonlinear uncertainty which instead of the external disturbance, the ambient noise is studied. As a restriction of the approach in [31], satisfying some of the conditions are necessary, which can reduce the applicability of the proposed scheme. On another side, in [31], during the sliding surface design, they neglect some of the system dynamic terms. To do this, a gain is considered in both the integral sliding mode surface and the sliding mode controller structures to attenuate the noise effects on the dynamics. The approach in [31] may lead to non-optimal sliding surface and then needs to more control effort to reach the sliding surface.. Since, utilizing SMC design requires a priori knowledge of the uncertainties, a new sliding mode back-stepping technique was proposed in [32] by combining sliding mode control design and the adaptive back-stepping technique with tuning functions to make ensure the movement of the tracking error will be along the sliding hyperplane. Besides, internal dynamic stability is a necessity for applying the SMC approach [33]; but, the system's zero dynamics stability seldom has been inspected in the literature.

Recently, to solve the robust performance control design problem, many back-stepping sliding mode controls (BSMCs) schemes through the combination of back-stepping control mechanism and SMC design have been developed, while the unmatched uncertainty generally was not considered [21], [22], [34]. In [22], for a knee exoskeleton used in order to assist human movement, a nonlinear disturbance observer was suggested and combined with a back-stepping sliding mode control. The approach in [22] had been used to reduce the influence of the modeling uncertainty and disturbance. In [21], an observer based backstepping terminal sliding mode controller for three degrees of freedom (DOF) robot manipulator was employed. In [34], using high-order extended state observer for the six DOF quadrotor unmanned aerial vehicle system, a BSMC algorithm was proposed to overcome the problems of the external wind disturbances and etc. Since, in the above-mentioned BSMC designs, the control system stability is strictly guaranteed in a step-by-step backstepping algorithm; therefore, the unstable zero dynamics effect on the system can be avoided. However, information about the parameter uncertainty and external disturbance upper bounds must be available to derive the switching gain of the BSMC; but, in most cases, such information cannot be obtained and if one uses a conservative method to make ensure the system stability by selecting a large switching gain, severe chattering may be occurred [35]. In other sides, H_2-characterization can be used in the SMC design to optimize the desired performance [36], [25]. In [36], a combination of the H_2-characterization and partial eigenstructure assignment was proposed to obtain the optimal gain of the conventional sliding surface for the linear system with matched uncertainty and external disturbances. In order to improve the buck converter robustness, a different hybrid H_2 model following control based on the digital redesign SMC approach was proposed in [25]. In addition, to improve the transient time performance, pole placement has been combined with H_2-characterization problem [37], [38]. In [37], an optimal control with H_2-characterization and regional pole constraint had been formulated using static state feedback. The design conditions were derived in terms of the LMIs and was employed on a power system model. In [38], for a small power system to be secured against inter-area modes, its controllers were designed with a mixed H_2/H_∞ optimization with regional pole placement.

The literature reviews show that the existing works tolerates from some practical issues in their design methods, i.e., poor transient response, practical aspects such as uncertainties and disturbances, and control effort. Thanks to fruitful TSFM representations of complex nonlinear systems, allows generalizing the well-known techniques in linear systems theory to nonlinear systems analysis and design. Transient response improvement for SMC-based nonlinear controller design is an interesting and challenging topic. Convex structure of TSFM representation of nonlinear systems provides us to design linear controller for the consequence subsystems optimally and then aggregate the controllers for the original nonlinear system. Moreover, elaborations of uncertainties and external disturbances, simultaneously, are another challenge topic for considering practical considerations in controller design.

In this paper, TSFM is used to describe a class of nonlinear systems with both the matched and the unmatched uncertainties. In this work, we suppose that the studied TSFM has an unknown bound of uncertainty and is exposed to an external disturbance. Therefore, as a well-known approach in robust control of nonlinear systems with bounded norm uncertainty, SMC has been utilized in this paper. Besides, due to the weakness of the SMC attenuation of the unmatched uncertainty as well as the matched uncertainty, by proposing new sliding surfaces to deal with both of the matched and the unmatched uncertainties, a new scheme of the SMC design based on the back-stepping procedure is proposed. Also, some adaptive laws are derived to estimate the bound of uncertainties. This paper aims to reduce the undeniable chattering phenomena in high frequency and tries to attenuate the external disturbance. In addition, in contrast to the previous works, we design an optimal sliding gain by considering all of the system specification, system limitation, and the required control effort to reach the desired transient time performance. To do this, first, the sliding surface and the optimal control input are defined such that they depend on the desired optimal state feedback gains. The optimal state feedback gains are designed such that the H_2-performance specification and α-stability condition are satisfied. Hence, in this paper to overcome the SMC weakness, a new robust control scheme is proposed to design an optimal dynamic BSMC for the nonlinear system described by TSFM. The main advantage and contribution of our proposed approach can be recounted as following:

1- An optimal and adaptive BSMC scheme is designed for a nonlinear system with all kinds of uncertainties and subjected to the external disturbance. To do this, we consider the H_2-performance problem specification and α-stability constraint during the sliding surface design. In addition, we propose a novel virtual control law to improve the robust performance of the nonlinear system.
2- The SMC design approaches usually suffer from knowing a prior knowledge about the bounds of the uncertainties. These bounds of the uncertainties are not available in many practical systems; therefore, to solve this, we derived some adaptive laws to estimate the unknown bounds of the uncertainties.
3- In this paper, we use the hyperbolic function instead of the signum function to reduce the chattering phenomena; i.e., $tanh(\cdot)$.

This paper is organized as follows: In Section II, a class of nonlinear system with the matched and the unmatched uncertainties based on TSFM description is introduced. In Section III, a novel sliding mode controller is proposed to be designed based on the back-stepping approach. In Section IV, first, new LMIs characterization for the H_2-problem and the α-stability constraint will be introduced to find optimal state feedback gain. Then, in the framework of the convex optimization problem, the optimal matrix gains of the sliding surface are designed. In Section V, to show the effectiveness of the proposed method, a two-link robot manipulator system is considered in a comparative example and the paper conclusion and future works are drawn in Section VI.

II. PROBLEM STATEMENT AND PRELIMINARIES

Consider a T-S fuzzy model of the nonlinear system with the matched and the unmatched uncertainties as follows:

$$\begin{aligned}\dot{x}_1(t) &= x_2(t) + d_1(x)\\ \dot{x}_2(t) &= \sum_{i=1}^{r} h_i(\mu)\left\{A_{s,i}x(t) + B_{1s,i}u(t)\right\} + d_2(x)\\ y(t) &= x_1(t)\\ z(t) &= \sum_{i=1}^{r} h_i(\mu)\left\{C_i x(t) + D_i u(t)\right\}\end{aligned} \tag{1}$$

where $x \in \mathbb{R}^n$, $u \in \mathbb{R}^m$, $y \in \mathbb{R}^{n_1}$ and $z \epsilon \mathbb{R}^q$ denote the state vector, the control input vector, the measured output vector, and the H_2-performance output vector, respectively. The state vector $x \in \mathbb{R}^n$ are defined as $x = \begin{bmatrix} x_1 & x_2 \end{bmatrix}^T$; $x_1 \in \mathbb{R}^{n_1}, x_2 \in \mathbb{R}^{n_2}$, $n_1 + n_2 = n$, and $n_1 = n_2$. Also, $d_1(x) \in \mathbb{R}^{n_1}$ and $d_2(x) \in \mathbb{R}^{n_2}$ denote the bounded matched and unmatched uncertainty with unknown bound, respectively. The system uncertainty satisfies the boundary conditions as $\left\|\dot{d}_1(x)\right\| < \delta_1 \|x(t)\|$, $\|d_2(x)\| < \delta_2 \|x(t)\|$, and $\|d_1(x)\| < \delta_3 \|x(t)\|$, where parameters δ_1, δ_2 and δ_3 are positive constants. $A_{s,i} \in \mathbb{R}^{n_2 \times n}$; $B_{1s,i} \in \mathbb{R}^{n_2 \times m}$; $C_i \in \mathbb{R}^{q \times n}$; $D_i \in \mathbb{R}^{q \times m}$ are the system matrices with appropriate dimensions. Also, $h_i(\mu)$ denotes the relative weighting value (normalized membership function), in which $h_i(\mu) \geq 0$ and $\sum_{i=1}^{r} h_i(\mu) = 1$. In this paper, we suppose that $q \leq m \leq \frac{n}{2}$. Using parallel distributed controller (PDC) [1] for the TSFM (1), the control input is considered as

$$u(t) = \sum\nolimits_{i=1}^{r} h_i(\mu) K_i x(t) \tag{2}$$

where K_i denotes the control input gain for the i^{th} fuzzy rule consequence subsystem, and $h_i(\mu)$ stands for the normalized membership function.

In this paper to handle both the matched and the unmatched uncertainties, first, the system states (1) are decoupled into the two subsystems as follows:

$$\dot{x}_1(t) = x_2(t) + d_1(x) \tag{3}$$

In subsystem (3), by considering the state variable $x_2(t)$ as a virtual control input, the matched uncertainty $d_1(x)$ can be handled by SMC approaches. Using system decomposition, the second subsystem is presented as follows:

$$\dot{x}_2(t) = \sum\nolimits_{i=1}^{r} h_i(\mu)\left\{A_{s,i}x(t) + B_{1s,i}u(t)\right\} + d_2(x) \tag{4}$$

where the matched uncertainty $d_2(x)$ can be handled by selecting an appropriate control input. We will aim to design a BSMC for dynamics (3)-(4) to achieve transient response improvement optimally and providing acceptable attenuation

level of the effects of the uncertainties and external disturbances. Moreover, practical issues are considered in the control effort design. Therefore, a multi-objective controller design is designed based on H_2-performance characterization and α-stability methods in the BSMC framework.

III. BACKSTEPPTING-BASED SLIDING MODE CONTROLLER DESIGN

In this section, a new approach to design SMC for the nonlinear system (1) is proposed. Since $y(t)$ is the measured output vector, consider $y_d(t)$ as the desired output vector, the output tracking error can be defined as $e_1(t) = x_1(t) - y_d(t)$. Hence, the first and the second time-derivatives of $e_1(t)$ are obtained as follows:

$$\begin{aligned}\dot{e}_1(t) &= \dot{x}_1(t) - \dot{y}_d(t) \\ &= x_2(t) + d_1(x(t)) - \dot{y}_d(t) \qquad (5)\\ \ddot{e}_1(t) &= \ddot{x}_1 - \ddot{x}_d = \dot{x}_2 - \ddot{y}_d \\ &= \sum_{i=1}^{r} h_i(\mu)\left\{A_{s,i}x(t) + B_{1s,i}u(t))\right\} + d_2(x) - \ddot{y}_d \qquad (6)\end{aligned}$$

Define $e_2 := \dot{e}_1$, the tracking error dynamics (5)-(6) can be rewritten as

$$\begin{aligned}\dot{e}_1 &= e_2 \qquad (7)\\ \dot{e}_2 &= \sum_{i=1}^{r} h_i(\mu)\left\{A_{s,i}x(t) + B_{1s,i}(u(t))\right\} + d_2(x) - \ddot{x}_d \qquad (8)\end{aligned}$$

Now, a sliding mode controller for the tracking error dynamic (7)-(8) will be designed based on the back-stepping approach in two steps. In the first step, a virtual controller is designed for (7). After that, in the second step, a controller is designed for (8), and consequently, for the overall output tracking error system.

Step1: Consider $x_2(t)$ as the virtual control input, then, (5) is rewritten as follows:

$$\dot{e}_1 = \dot{x}_1 - \dot{y}_d = x_{2d} + d_1(x) - \dot{y}_d \qquad (9)$$

where $x_{2d}(t) = \alpha(e_1(t)) + \dot{y}_d - \int_0^t \hat{\rho}_1 sgn(\sigma_1)\, d\tau$ stands the virtual control input to be obtained such that the first state vector $e_1(t)$ reaches to zero at finite-time in the presence of the uncertainty $d_1(x)$. To do this, consider the sliding surface for (9) as follows:

$$\sigma_1 = S(\dot{e}_1 + k_1 e_1) \qquad (10)$$

where $S \in \mathbb{R}^{m\times n_1}$ and $k_1 \in \mathbb{R}$, $k_1 > 0$ are the sliding gains to be obtained. Moreover, the switching matrix gain is defined as $S = \sum_{i=1}^{r} h_i(\mu) S_i(\mu)$. One can select the virtual control input as

$$x_{2d}(t) = \alpha(e_1(t)) + \dot{y}_d - \int_0^t \hat{\rho}_1 sign(\sigma_1)\, d\tau$$

where $\alpha(e_1(t)) = -k_1 e_1(t)$, and show that the system dynamic (9) will be asymptotically stable using the virtual control input $x_{2d}(t)$.

Now, the sliding surface (10) can be rewritten as

$$\begin{aligned}\sigma_1 &= S(\dot{e}_1 + k_1 e_1) \\ &= S(x_{2d}(t) + d_1(x) - \dot{y}_d + k_1 e_1) \\ &= S(-k_1 e_1(t) + \dot{y}_d - \int_0^t \hat{\rho}_1 sign(\sigma_1)\, d\tau \\ &\quad + d_1(x) + k_1 e_1 - \dot{y}_d) \\ &= S\left(-\int_0^t \hat{\rho}_1 sign(\sigma_1)\, d\tau + d_1(x)\right) \qquad (11)\end{aligned}$$

The bound of uncertainty can be calculated by proposing the constant bound as $\rho_1 = \epsilon_1 + \delta_1 \|x(t)\|$, where ϵ_1 is a known positive small scalar value.

To estimate the bound $\hat{\rho}_1$, define $\tilde{\delta}_1 = \hat{\delta}_1 - \delta_1$ as the error between the estimated and the true values of the coefficient in the uncertainty bound equation. Then, the estimated bound of the uncertainty and the coefficient are obtained as

$$\begin{aligned}\hat{\rho}_1 &= \epsilon_1 + \hat{\delta}_1 \|x(t)\| \\ \dot{\hat{\delta}}_1 &= \eta_1 \|\sigma_1\| \|S\| \|x(t)\| \qquad (12)\end{aligned}$$

where η_1 is an arbitrary small positive constant value.

Lemma 1: The tracking error trajectory (9) *is asymptotically stable using* $x_{2d}(t) = -k_1 e_1(t) - \int_0^t \hat{\rho}_1 tanh(\sigma_1)\, d\tau$ *with parameters update rule given in* (12).

Proof: Consider the Lyapunov function candidate as follows:

$$V_1 = \frac{1}{2}(\sigma_1)^T(\sigma_1) + \frac{1}{2\eta_1}(\tilde{\delta}_1)^2 \qquad (13)$$

Take the time-derivative on (13), one has

$$\begin{aligned}\dot{V}_1 &= \sigma_1^T \dot{\sigma}_1 + \frac{1}{\eta}\tilde{\delta}_1\dot{\tilde{\delta}}_1 \\ &= (\sigma_1)^T S\left(-\hat{\rho}_1 sign(\sigma_1) + \dot{d}_1(x)\right) + \frac{1}{\eta_1}\tilde{\delta}_1\dot{\tilde{\delta}}_1 \\ &= \left(-\hat{\rho}_1 (\sigma_1)^T S sign(\sigma_1) + (\sigma_1)^T S\dot{d}_1(x)\right) + \frac{1}{\eta_1}\tilde{\delta}_1\dot{\tilde{\delta}}_1 \\ &= -\hat{\rho}_1 |\sigma_1| S + (\sigma_1)^T S\dot{d}_1(x) + \frac{1}{\eta_1}\tilde{\delta}_1\dot{\tilde{\delta}}_1 \\ &\le -\hat{\rho}_1 S\|\sigma_1\| + |\sigma_1||S|\left|\dot{d}_1(x)\right| + \frac{1}{\eta_1}\tilde{\delta}_1\dot{\tilde{\delta}}_1 \\ &\le -\hat{\rho}_1 S\|\sigma_1\| + \|\sigma_1\|\|S\|\left\|\dot{d}_1(x)\right\| + \frac{1}{\eta_1}\tilde{\delta}_1\dot{\tilde{\delta}}_1 \\ &< -\|\sigma_1\|\|S\|\left(\hat{\rho}_1 - \delta_1\|x(t)\|\right) + \frac{1}{\eta_1}\tilde{\delta}_1\dot{\tilde{\delta}}_1 \qquad (14)\end{aligned}$$

Substitute $\hat{\rho}_1$ from (12) in (14) yields

$$\begin{aligned}\dot{V}_1 &< -\epsilon_1\|\sigma_1\|\|S\| - \|\sigma_1\|\|S\|\left(\hat{\delta}_1 - \delta_1\right)\|x(t)\| + \frac{1}{\eta_1}\tilde{\delta}_1\dot{\tilde{\delta}}_1 \\ &= -\epsilon\|\sigma_1\|\|S\| - \|\sigma_1\|\|S\|\|x(t)\|\tilde{\delta}_1 + \frac{1}{\eta_1}\tilde{\delta}_1\dot{\tilde{\delta}}_1 \qquad (15)\end{aligned}$$

Substitute $\dot{\tilde{\delta}}_1$, given in (12), in (15) yields

$$\dot{V}_1 < -\epsilon_1 \|\sigma_1\| \|S\| < 0 \tag{16}$$

From (16), the proof is completed. ■

Step2: Since the $x_2(t)$ is not necessarily available, we propose the new variable $z_1(t) = x_2(t) - x_{2d}(t)$ as the difference between $x_2(t)$ and the desired virtual control input. Also, we define $\tilde{\delta}_2 = \hat{\delta}_2 - \delta_2$ and $\tilde{\delta}_3 = \hat{\delta}_3 - \delta_3$ as the difference between the estimated and the true values of the upper-bounds of both uncertainties; i.e., $d_2(x)$ and $d_1(x)$. Then, for $d_2(x)$, the estimated upper-bound and parameter adaption law are obtained as follows:

$$\begin{aligned} \hat{\rho}_2 &= \epsilon_2 + \hat{\delta}_2 \|x(t)\| \\ \dot{\hat{\delta}}_2 &= \eta_2 \|\sigma_2\| \|S\| \|x(t)\| \end{aligned} \tag{17}$$

where η_2 is an arbitrary small positive constant value. In addition, the estimated upper-bound and parameter adaption law for $d_1(x)$ are obtained as

$$\begin{aligned} \hat{\rho}_3 &= \epsilon_3 + \hat{\delta}_3 \|x(t)\| \\ \dot{\hat{\delta}}_3 &= k_1 \eta_3 \|\sigma_2\| \|S\| \|x(t)\| \end{aligned} \tag{18}$$

where η_3 is an arbitrary small positive constant value, and k_1 is the same as the constant value in (10) which to be designed.

Now, consider a traditional sliding surface for the system dynamics (4) as follows:

$$\sigma_2 = S(x_2(t) - x_{2d}(t)) \tag{19}$$

Theorem 1 shows that the error $e_2(t)$ in (8) converges to origin with the control input $u(t)$ as follows:

$$\begin{aligned} u(t) = &-(SB_{1s})^{-1} S(\sum_{i=1}^{r} h_i(\mu) \{A_{s,i}x(t)\} - k_1^2 x_1(t) \\ &+ \ddot{y}_d - k_1 \left(\int_0^t \hat{\rho}_1 sign(\sigma_1) d\tau + \hat{\rho}_3 sign(\sigma_2) \right) \\ &+ \hat{\rho}_1 sign(\sigma_1) + \hat{\rho}_2 sign(\sigma_2) + k_2 z_1(t)) \end{aligned} \tag{20}$$

where $K_2 \in \mathbb{R}$, $K_2 > 0$, and $h_i(\mu)$ are the normalized fuzzy membership functions defined in (1)-(2).

Theorem 1: The tracking error dynamics (8) is asymptotically stable using the control input (20) and parameters updating rules (17)-(18).

Proof: Select the Lyapunov candidate as follows:

$$\begin{aligned} V_2 = &\frac{1}{2} (S(x_2(t) - x_{2d}(t)))^T (S(x_2(t) - x_{2d}(t))) \\ &+ \frac{1}{2\eta_3} (\tilde{\delta}_3)^2 + \frac{1}{2\eta_2} (\tilde{\delta}_2)^2 \end{aligned} \tag{21}$$

Time-derivative of $z_1(t)$ is obtained as

$$\begin{aligned} \dot{z}_1(t) &= \dot{x}_2(t) - \dot{x}_{2d}(t) \\ &= \dot{x}_2(t) - \frac{\partial \left(-k_1 x_1(t) + \dot{y}_d - \int_0^t \hat{\rho}_1 sign(\sigma_1) d\tau \right)}{\partial t} \\ &= \dot{x}_2(t) + k_1 \dot{x}_1(t) - \ddot{y}_d + \hat{\rho}_1 sign(\sigma_1) \end{aligned} \tag{22}$$

Substituting $\dot{x}_2(t)$ and $\dot{x}_1(t) = x_{2d}(t) + d_1(x)$ in (22), one has

$$\begin{aligned} \dot{z}_1(t) = &\sum_{i=1}^{r} h_i(\mu) \{A_{s,i}x(t) + B_{1s,i}u(t)\} + d_2(x) \\ &+ k_1(-k_1 x_1(t) - \int_0^t \hat{\rho}_1 sign(\sigma_1) d\tau \\ &+ d_1(x)) - \ddot{y}_d + \hat{\rho}_1 sign(\sigma_1) \end{aligned} \tag{23}$$

Now, using (23), time-derivative of (21) is obtained as

$$\begin{aligned} \dot{V}_2 = &\frac{1}{2} (Sz_1)^T (S\dot{z}_1) + \frac{1}{2} (S\dot{z}_1)^T (Sz_1) \\ &+ \frac{1}{\eta_3} \tilde{\delta}_3 \dot{\tilde{\delta}}_3 + \frac{1}{\eta_2} \tilde{\delta}_1 \dot{\tilde{\delta}}_1 \\ = &(\sigma_2)^T S(\sum_{i=1}^{r} h_i(\mu) \{A_{s,i}x(t) + B_{1s,i}u(t)\} + d_2(x) \\ &- \ddot{y}_d + \frac{1}{\eta_1} \tilde{\delta}_3 \dot{\tilde{\delta}}_3 + \frac{1}{\eta_2} \tilde{\delta}_2 \dot{\tilde{\delta}}_2 + k_1(-k_1 x_1(t) \\ &- \int_0^t \hat{\rho}_1 sign(\sigma_1) d\tau + d_1(x)) + \hat{\rho}_1 sign(\sigma_1)) \end{aligned} \tag{24}$$

Substituting the control input (20) with $k_2 > 0$ in (24), one has

$$\begin{aligned} \dot{V}_2 = &(Sz_1)^T (-Sk_2 z_1(t) - S(\hat{\rho}_2 + K_1 \hat{\rho}_3) sign(\sigma_2) \\ &+ Sd_2(x) + Sk_1 d_1(x)) + \frac{1}{\eta_3} \tilde{\delta}_1 \dot{\tilde{\delta}}_1 + \frac{1}{\eta_2} \tilde{\delta}_2 \dot{\tilde{\delta}}_2 \\ = &-k_2 (\sigma_2)^T (\sigma_2) + (\sigma_2)^T (-S(\hat{\rho}_2 + K_1 \hat{\rho}_3) sign(\sigma_2) \\ &+ Sd_2(x) + Sk_1 d_1(x)) + \frac{1}{\eta_3} \tilde{\delta}_3 \dot{\tilde{\delta}}_3 + \frac{1}{\eta_2} \tilde{\delta}_2 \dot{\tilde{\delta}}_2 \\ \leq &-k_2 \|\sigma_2\|^2 + (-|\sigma_2| |S| (\hat{\rho}_2 + K_1 \hat{\rho}_3) + \frac{1}{\eta_2} \tilde{\delta}_2 \dot{\tilde{\delta}}_2 \\ &+ \frac{1}{\eta_3} \tilde{\delta}_3 \dot{\tilde{\delta}}_3 + |\sigma_2| |S| |d_2(x)| + k_1 |\sigma_2| |S| |d_1(x)|) \\ \leq &-k_2 \|\sigma_2\|^2 + (-\|\sigma_2\| \|S\| (\hat{\rho}_2 + K_1 \hat{\rho}_3) \\ &+ \|\sigma_2\| \|S\| \|d_2(x)\| + k_1 \|\sigma_2\| \|S\| \|d_1(x)\|) \\ &+ \frac{1}{\eta_3} \tilde{\delta}_3 \dot{\tilde{\delta}}_3 + \frac{1}{\eta_2} \tilde{\delta}_2 \dot{\tilde{\delta}}_2 \\ \leq &-k_2 \|\sigma_2\|^2 + (-\|\sigma_2\| \|S\| (\hat{\rho}_2 + K_1 \hat{\rho}_3) \\ &+ \|\sigma_2\| \|S\| \|d_2(x)\| + k_1 \|\sigma_2\| \|S\| \|d_1(x)\|) \\ &+ \frac{1}{\eta_3} \tilde{\delta}_3 \dot{\tilde{\delta}}_3 + \frac{1}{\eta_2} \tilde{\delta}_2 \dot{\tilde{\delta}}_2 \\ < &-k_2 \|\sigma_2\|^2 + (-\|\sigma_2\| \|S\| (\hat{\rho}_2 + K_1 \hat{\rho}_3) \\ &+ \delta_2 \|\sigma_2\| \|S\| \|x(t)\| + k_1 \delta_3 \|\sigma_2\| \|S\| \|x(t)\|) \\ &+ \frac{1}{\eta_3} \tilde{\delta}_3 \dot{\tilde{\delta}}_3 + \frac{1}{\eta_2} \tilde{\delta}_2 \dot{\tilde{\delta}}_2 \end{aligned} \tag{25}$$

Substitute $\hat{\rho}_2$ and $\hat{\rho}_3$, given in (17) and (18), in (25), one has

$$\begin{aligned} \dot{V}_2 < &-k_2 \|\sigma_2\|^2 - (\epsilon_2 + k_1 \epsilon_3) \|\sigma_2\| \|S\| \|x(t)\| \\ &+ \|\sigma_2\| \|S\| \|x(t)\| (\delta_2 + k_1 \delta_3 - \hat{\delta}_2 - k_1 \hat{\delta}_3) \\ &+ \frac{1}{\eta_3} \tilde{\delta}_3 \dot{\tilde{\delta}}_3 + \frac{1}{\eta_2} \tilde{\delta}_2 \dot{\tilde{\delta}}_2 \end{aligned} \tag{26}$$

Substitute $\dot{\bar{\delta}}_2$ and $\dot{\bar{\delta}}_3$, given in (17) and (18), in (26), one has

$$\dot{V}_2 < -k_2 \|\sigma_2\|^2 - (\epsilon_2 + k_1\epsilon_3) \|\sigma_2\| \|S\| \|x(t)\| < 0 \quad (27)$$

which the reachability conditions hold and the proof is completed. ∎

In this paper, to reduce the chattering phenomena [39], we use hyperbolic function instead of signum function; i.e., $tanh(\sigma_1)$, $tanh(\sigma_2)$. Therefore, the control input (20) is rewritten as

$$\begin{aligned} u(t) = &-(SB_{1s})^{-1} S(\sum_{i=1}^{r} h_i(\mu) \{A_{s,i}x(t)\} + \ddot{y}_d \\ &- k_1^2 x_1(t) - k_1(\int_0^t \hat{\rho}_1 tanh(\sigma_1)\, d\tau + \hat{\rho}_3 tanh(\sigma_2)) \\ &+ \hat{\rho}_1 tanh(\sigma_1) + \hat{\rho}_2 tanh(\sigma_2) + k_2 z_1(t)). \end{aligned} \quad (28)$$

IV. OPTIMAL SLIDING MODE CONTROLLER DESIGN

In this section, for the nonlinear system (1) which can be exposed to an external disturbance, an optimal controller is designed. To do this, first, we consider the TSFM (1) subjected to the external disturbance $w(t)$. Therefore, we design a multi-objective state feedback control by incorporating of (*i*) the regional pole placement constraint, and (*ii*) the H_2-characterization problem both for the consequence linear local subsystems. The H_2 optimization provides the minimization of the effect of the disturbance w upon the H_2-performance output vector z, while the additional uncertainties are neglected, i.e., $d_1(x) = 0$ and $d_2(x) = 0$. Therefore, for the TSFM (1) subjected to the external disturbance, we design the adaptive and optimal BSMC gains in the control law (28).

The T-S fuzzy model (1), is rewritten as

$$\begin{aligned} \dot{x}(t) &= Ax(t) + B_1 u(t) + B_2 w(t) + d(x) \\ y(t) &= x_1(t) \\ z(t) &= \sum_{i=1}^{r} h_i(\mu) \{C_i x(t) + D_i u(t)\} \end{aligned} \quad (29)$$

where

$$A = \sum_{i=1}^{r} h_i(\mu) \begin{bmatrix} 0_{n_1 \times n_1} & I_{n_2 \times n_2} \\ A_{1,i} & A_{2,i} \end{bmatrix},$$

$$B_1 = \sum_{i=1}^{r} h_i(\mu) \begin{bmatrix} 0_{n_1 \times m} \\ B_{1s,i} \end{bmatrix},$$

and $w \in \mathbb{R}^q$ denotes the external disturbance input, while its input matrix gain B_2 has an appropriate dimension, and $d(x) = \sum_{i=1}^{r} h_i(\mu) \begin{bmatrix} d_1(x) \\ d_2(x) \end{bmatrix}$.

To design the multi-objective optimal BSMC control, consider the TSFM (29) with no additional uncertainty as

$$\begin{aligned} \dot{x}(t) &= Ax(t) + B_1 u(t) + B_2 w(t)\, y(t) = x_1(t) \\ z(t) &= \sum_{i=1}^{r} h_i(\mu) \{C_i x(t) + D_i u(t)\} \end{aligned} \quad (30)$$

In lemma 2, for the TSFM (30), using LMI characterization, an H_2 performance from the disturbance input w to the output z is considered.

Lemma 2: For the nonlinear system (30), the following statements are equivalent:

a) *$\exists K_j, j = 1, \ldots, r$, such that $A_i + B_{1,i}K_j$ is stable and the H_2 performance from the disturbance w to the output z is less than γ.*

$$\sum_{i=1}^{r}\sum_{j=1}^{r} h_i h_j (\| (C_i + D_i K_j) \times [SI - (A_i + K_j)]^{-1} B_{2,i} \|_2^2) < \gamma \quad (31)$$

b) *$\exists X > 0$ and $Z > 0$ such that*

$$\sum_{i=1}^{r}\sum_{j=1}^{r} h_i h_j \begin{bmatrix} A_i X + B_{1,i}Y_j + XA_i^T + Y_j^T B_{1,i}^T & * \\ C_i X + D_i Y_j & -\gamma I \end{bmatrix} < 0 \quad (32)$$

$$\sum_{i=1}^{r} h_i \left(\begin{bmatrix} -Z & * \\ B_{2,i} & -X \end{bmatrix} \right) < 0 \quad (33)$$

$$trace(Z) < 1 \quad (34)$$

where $Y_j = K_j X$.

c) *$\exists X > 0, Z > 0$ and nonsingular matrix G such that*

$$\sum_{i=1}^{r}\sum_{j=1}^{r} h_i h_j \begin{bmatrix} -(G+G^T) & * & * \\ A_i G + B_{1,i}Y_j + X + G & -2X & * \\ C_i G + D_i Y_j & 0 & -\gamma I \end{bmatrix} < 0 \quad (35)$$

$$\sum_{i=1}^{r}\sum_{j=1}^{r} h_i h_j \left(\begin{bmatrix} X & * \\ B_{2,i}^T & Z \end{bmatrix} \right) < 0 \quad (36)$$

$$trace(Z) < 1 \quad (37)$$

where $Y_j = K_j G$ and $X > 0, Z > 0$ are positive definite matrices and G is a general nonsingular matrix variable.

Proof: Note that parts (a & b) are equivalent forms of the standard H_2 state-feedback synthesis which is developed by Lemma (1) in [40] for the T-S fuzzy system. To prove part (c), it is based on a convex combination upon the extended H_2-characterization suggested in [41]. The H_2-characterization can be rewritten [41] for each consequence linear subsystem (30) as

$$\begin{bmatrix} -(G+G^T) & * & * & * \\ A_i G + B_{1,i}Y_j + X & -X & * & * \\ C_i G + D_i Y_j & 0 - \gamma I & * & \\ G & 0 & 0 & -X \end{bmatrix} < 0 \quad (38)$$

$$\begin{bmatrix} X & * \\ B_{2,i}^T & Z \end{bmatrix} < 0 \quad (39)$$

$$trace(Z) < 1 \quad (40)$$

Using Schur complement, (38) is rewritten as

$$\begin{bmatrix} -(G + G^T) + G^T X^{-1} G & * & * \\ A_i G + B_{1,i}Y_j + X & -X & * \\ C_i G + D_i Y_j & 0 & -\gamma I \end{bmatrix} < 0 \quad (41)$$

$$\begin{bmatrix} -\left(\mathrm{G}+\mathrm{G}^T\right)+\mathrm{G}^T X^{-1}\mathrm{G} & * \\ A_i\mathrm{G}+B_{1,i}Y_j+X & -X \end{bmatrix} + \gamma^{-1}\begin{bmatrix} (C_i\mathrm{G}+D_iY_j)^T \\ 0 \end{bmatrix}\begin{bmatrix} C_i\mathrm{G}+D_iY_j & 0 \end{bmatrix} < 0 \quad (42)$$

$$\begin{bmatrix} -\left(\mathrm{G}+\mathrm{G}^T\right) & * \\ A_i\mathrm{G}+B_{1,i}Y_j+X+\mathrm{G} & -2X \end{bmatrix} + \gamma^{-1}\begin{bmatrix} (C_i\mathrm{G}+D_iY_j)^T \\ 0 \end{bmatrix}\begin{bmatrix} C_i\mathrm{G}+D_iY_j & 0 \end{bmatrix} < 0 \quad (43)$$

Then, using the fuzzy aggregation, the overall H_2-characterization can be reached as in (35)-(37). The proof is completed. ■

Remark 1: Defining $M_{i,j}$ and $N_{i,j}$ as

$$M_{ij} = \begin{bmatrix} -\left(\mathrm{G}+\mathrm{G}^T\right) & * & * \\ A_i\mathrm{G}+B_{1,i}Y_j+X+\mathrm{G} & -2X & * \\ C_i\mathrm{G}+D_iY_j & 0 & -\gamma I \end{bmatrix}$$
$$N_{ij} = \begin{bmatrix} X & * \\ B_{2,i}^T & Z \end{bmatrix} \quad (44)$$

Then, in term of the new variables (44), *one may rewrite the LMIs* (35)-(37) *as*

$$\sum_{i=1}^{r}\sum_{j=1}^{r} h_i h_j M_{ij} < 0 \quad (45)$$

$$\sum_{i=1}^{r}\sum_{j=1}^{r} h_i h_j N_{ij} < 0 \quad (46)$$

$$trace\,(Z) < 1 \quad (47)$$

where (44)-(47) are the parameters-varying matrix inequality.

From[40], one may conclude that the following LMIs are sufficient conditions to satisfy the LMIs (45)-(47):

$$\begin{aligned} M_{ii} &< 0,\ \frac{1}{r-1}M_{ii}+\frac{1}{2}\left(M_{ij}+M_{ji}\right) \\ &< 0;\ i,j=1,\ldots,r;\ i\neq j \\ N_{ii} &< 0,\ \frac{1}{r-1}N_{ii}+\frac{1}{2}\left(N_{ij}+N_{ji}\right) \\ &< 0;\ i,j=1,\ldots,r;\ i\neq j\ trace(Z)<1. \end{aligned} \quad (48)$$

In addition, to improve the transient response performance of the control system, the α-stability object is incorporated in the LMI framework in the following lemma.

Lemma 3: For the nonlinear system (30), *the following statements are equivalent:*

1) *For* $i,j=1,\ldots,r$

$$(A_i+B_{1,i}K_j)X+X(A_i+B_{1,i}K_j)^T+2\alpha X<0 \quad (49)$$

2) $\exists X>0, \left(G+G^T\right)>0$ *and nonsingular matrix* Y_j *such that*

$$\sum_{i=1}^{r}\sum_{j=1}^{r} h_i h_j \begin{bmatrix} -\left(G+G^T\right) & * & * \\ X+G+A_iG+B_{1,i}Y_j & -2X & * \\ \sqrt{2\alpha}G & 0 & -X \end{bmatrix} < 0; \quad (50)$$

Proof: Using Schur complement lemma, (50) can be rewritten for each consequence subsystem as

$$\begin{bmatrix} -\left(G+G^T\right)+2\alpha G^T X^{-1}G & * \\ X+G+A_iG+B_{1,i}Y_j & -2X \end{bmatrix} < 0 \quad (51)$$

which $G+G^T>0$. Applying the congruence transformation by $\begin{bmatrix} G^{-T} & 0 \\ 0 & X^{-1} \end{bmatrix}$ in (51), results in

$$\begin{bmatrix} -\left(\tilde{G}+\tilde{G}^{\mathrm{T}}\right)+2\alpha\tilde{X} & * \\ \tilde{X}A_i+\tilde{X}B_{1,i}K_j+\tilde{X}+\tilde{G} & -2\tilde{X} \end{bmatrix} < 0 \quad (52)$$

where $\tilde{G}=\tilde{G}^{-1}, \tilde{X}=X^{-1}$, and $K_{\mathrm{j}}=Y_jG^{-1}$. Then (52) can be rewritten as

$$\begin{bmatrix} 2\alpha\tilde{X} & * \\ \tilde{X}A_i+\tilde{X}B_{1,i}K_j+\tilde{X} & -2\tilde{X} \end{bmatrix} + herm(\begin{bmatrix} -I \\ I \end{bmatrix}\tilde{G}^T\begin{bmatrix} I & 0 \end{bmatrix}) < 0 \quad (53)$$

Employing the Projection lemma, (53) holds if the following inequalities are satisfied

$$\begin{bmatrix} I \\ I \end{bmatrix}^T\begin{bmatrix} 2\alpha\tilde{X} & * \\ \tilde{X}A_i+\tilde{X}B_{1,i}K_j+\tilde{X} & -2\tilde{X} \end{bmatrix}\begin{bmatrix} I \\ I \end{bmatrix} < 0 \quad (54)$$

$$\begin{bmatrix} 0 \\ I \end{bmatrix}^T\begin{bmatrix} 2\alpha\tilde{X} & * \\ \tilde{X}A_i+\tilde{X}B_{1,i}K_j+\tilde{X} & -2\tilde{X} \end{bmatrix}\begin{bmatrix} 0 \\ I \end{bmatrix} < 0 \quad (55)$$

Inequality (55) indicates $-\tilde{X}<0$ and (54) is equivalent to

$$\tilde{X}(A_i+B_{1,i}K_j)+(A_i+B_{1,i}K_j)^T\tilde{X}+2\alpha\tilde{X}<0 \quad (56)$$

Pre- and post-multiplying $X=\tilde{X}^{-1}$ in (58), yields

$$(A_i+B_{1,i}Y_j)X+X(A_i+B_{1,i}Y_j)^T+2\alpha X<0 \quad (57)$$

where $Y_j = K_{\mathrm{j}}X$. Employing Schur complement lemma on (57), shows that it is equivalent to (49). The proof is completed. ■

To design the multi-objective state feedback control and to achieve the transient performance improvement and disturbance attenuation objects concurrently, the following generalized eigenvalue problem (GEVP) is proposed:

$$\begin{aligned} &minimize\ \gamma \\ &subject\ \ to \\ &\qquad (37)\,,(38)\,,(39)\ and\ (50)\ for\ (30)\,. \end{aligned} \quad (58)$$

To obtain the sliding gain S in (10), the j^{th} sliding gain S_j is calculated from the following equation

$$-\left(S_jB_{1s,j}\right)^{-1}\left(S_j\left[A_{1,j}-(k_1-k_2)\,k_1\ A_{2,j}+k_2\right]x + S_j\ddot{y}_d\right) = K_{\mathrm{j}}x, for j=1,\ldots,r \quad (59)$$

Suppose that $S_j = B_{1s,j}^T P_j$, where P_j are positive definite matrices. Assume that $S_jB_{1\mathrm{s,j}}$ is invertible. If $S_jB_{1\mathrm{s,j}}$ is not invertible, one may use regularization approach [42], [43] to proceed the design procedure. Then, to obtain P_j,

Algorithm 1 The Pseudo-Code of the Proposed Control System Design Procedure

(1) Initialize the small arbitrary values for the updating rules (12) and (17)-(18) parameters; i.e. $\boldsymbol{\varepsilon}$, $\boldsymbol{\eta_1}$, $\boldsymbol{\eta_2}$, $\boldsymbol{\eta_3}$, and $\boldsymbol{k_1}$.
(2) Initialize the control input (20) parameter $\boldsymbol{k_2 > 0}$; e.g. $\boldsymbol{k_2 = 2k_1}$.
(3) Solve GEVP (58), to obtain $\boldsymbol{Y_j}$ and $\boldsymbol{G_j}$, and then, $\boldsymbol{K_j = Y_j G_j^{-1}}$.
% Optimal sliding mode control design
(4) Solve GEVP (61).
(5) Obtain $\boldsymbol{S_i = B_{1,j}^T P_j}$.
(6) Calculate the switching matrix gain $\boldsymbol{S = \sum_{i=1}^{r} h_i(\mu) S_i(\mu)}$.
(7) Define the switching surface (10) as $\boldsymbol{\sigma_1 \triangleq S(\dot{e}_1 + k_1 e_1)}$.
(8) Define the virtual control input as $\boldsymbol{x_{2d}(t) \triangleq -k_1 e_1(t) - \int_0^t \hat{\rho}_1 tanh(\sigma_1) d\tau}$.
(9) Define the switching surface (19) as $\boldsymbol{\sigma_2 \triangleq S(x_2(t) - x_{2d}(t))}$.
(10) Generate the control law $\boldsymbol{u(t)}$ from (28). (11) Update the adaptive parameter estimation by (12) and (17)-(18).
(12) GOTO step 7.

using a simple relaxation method, (59) can be rewritten as

$$\begin{aligned} &minimize\ \delta_j \\ &subject\ \ to \\ &\left\| \left(B_1^T P_j \left(A_{\lambda,j} x + \ddot{y}_d - B_{1,j} K_j x \right) \right) \right\| < \delta_j, \\ &for\ j = 1, \ldots, r \end{aligned} \tag{60}$$

where $A_{\lambda,j} = \left[A_{1,j} - (k_1 - k_2)\, k_1 \ A_{2,j} + k_2 \right]$, $\delta_j > 0$, and K_j are the j^{th} state-feedback gains in (2).

Using Schur complement lemma, the GEVP problem (60) is rewritten as follows:

$$\begin{aligned} &minimise\ \delta_j \\ &subject\ \ to \\ &\begin{bmatrix} -\delta_j I & * \\ B_{1,j}^T P_j (A_{\lambda,j} x + \ddot{y}_d - B_{1,j} K_j x) & -\delta_j I \end{bmatrix} < 0, \\ &for\ j = 1, \ldots, r \end{aligned} \tag{61}$$

The summary of the proposed design procedure is illustrated by Algorithm 1.

V. SIMULATION RESULTS

To evaluate the effectiveness of the proposed approach a two-link robot system is studied. Consider the two-link robot system depicted in Fig. 1, where $f_1(x), f_2(x), g_{11}(x), g_{12}(x)$, $g_{21}(x)$, and $g_{22}(x)$ have been defined in [44]. $x_1 = q_1$ and $x_2 = q_2$ are the angular positions, m_1 and m_2 are the link masses, l_1, and l_2 are the links length, $\left[\tau_1 \ \tau_2 \right]^T$ are the applied torques. The equations of the two-link robot

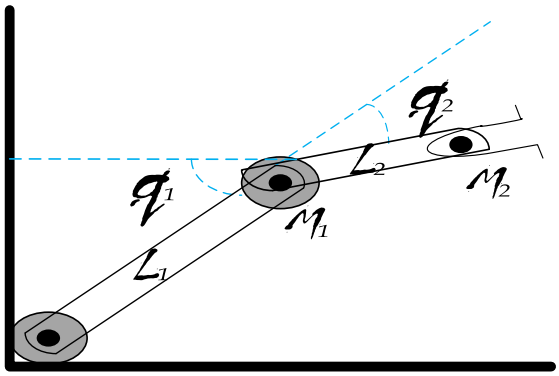

FIGURE 1. A two-link robot manipulator configuration.

manipulator are expressed as [41]

$$\begin{aligned} \dot{x}_1 &= x_2 + d_{11}(x) + w_1 \\ \dot{x}_2 &= = f_1(x) + g_{11}(x)\tau_1 + g_{12}(x)\tau_2 + d_{21}(x) + w_2 \\ \dot{x}_3 &= x_4 + d_{12}(x) + w_3 \\ \dot{x}_4 &= f_2(x) + g_{21}(x)\tau_1 + g_{22}(x)\tau_2 + d_{22}(x) + w_4 \\ y_1 &= x_1, y_2 = x_3, z = x_1 + x_3, \end{aligned} \tag{62}$$

where $d(x) = [d_{11}(x), d_{21}(x), d_{12}(x), d_{21}(x)]^T$ and $w(t) = [w_1, w_2, w_3, w_4]^T$ denote the additional/ unmatched uncertainty and the external disturbance, respectively.

The TSFM matrices of (62) with 9 rules are as follows [44]:

$$A_1 = \begin{bmatrix} 0.000 & 1.000 & 0.000 & 0.00 \\ 5.927 & -0.001 & -0.315 & -8.4 \times 10^{-6} \\ 0.000 & 0.000 & 0.000 & 1.00 \\ -6.859 & 0.002 & 3.155 & 6.2 \times 10^{-6} \end{bmatrix},$$

$$A_2 = \begin{bmatrix} 0.0000 & 1.0000 & 0.0000 & 0.0000 \\ 3.0428 & -0.0011 & 0.1791 & -0.0002 \\ 0.0000 & 0.0000 & 0.0000 & 1.0000 \\ 3.5436 & 0.0313 & 2.5611 & 1.14 \times 10^{-5} \end{bmatrix},$$

$$A_3 = \begin{bmatrix} 0.0000 & 1.0000 & 0.0000 & 0.0000 \\ 6.2728 & 0.0030 & 0.4339 & -0.0001 \\ 0.0000 & 0.0000 & 0.0000 & 1.0000 \\ 9.1041 & 0.0158 & -1.0574 & -3.2 \times 10^{-5} \end{bmatrix},$$

$$A_4 = \begin{bmatrix} 0.0000 & 1.0000 & 0.0000 & 0.0000 \\ 6.4535 & 0.0017 & 1.2427 & 0.0002 \\ 0.0000 & 0.0000 & 0.0000 & 1.0000 \\ -3.1873 & -0.0306 & 5.1911 & -1.8 \times 10^{-5} \end{bmatrix},$$

$$A_5 = \begin{bmatrix} 0.0000 & 1.0 & 0.0000 & 0.0 \\ 11.1336 & 0.0 & -1.8145 & 0.0 \\ 0.0000 & 0.0 & 0.0000 & 1.0 \\ -9.0918 & 0.0 & 9.1638 & 0.0 \end{bmatrix},$$

$$A_6 = \begin{bmatrix} 0.0000 & 1.0000 & 0.0000 & 0.0000 \\ 6.1702 & -0.0011 & 1.6870 & -0.0002 \\ 0.0000 & 0.0000 & 0.0000 & 1.0000 \\ -2.3559 & 0.0314 & 4.5298 & 1.1 \times 10^{-5} \end{bmatrix},$$

$$A_7 = \begin{bmatrix} 0.0000 & 1.0000 & 0.0000 & 0.0000 \\ 6.2728 & -0.0041 & 0.6205 & 0.0001 \\ 0.0000 & 0.0000 & 0.0000 & 1.0000 \\ 8.8794 & -0.0193 & -1.0119 & 4.4 \times 10^{-5} \end{bmatrix},$$

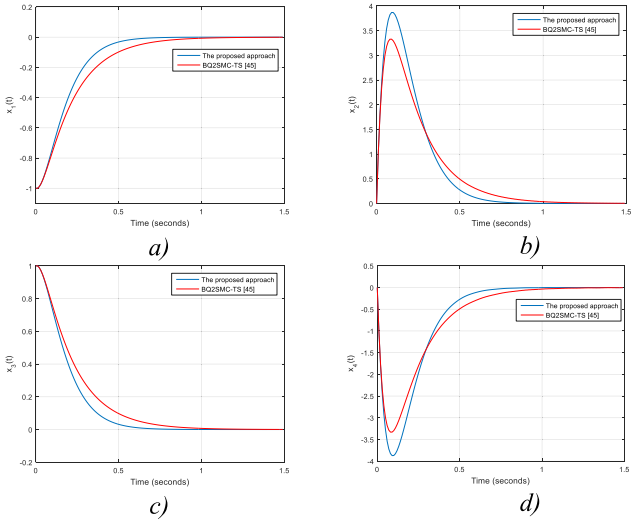

FIGURE 2. Responses of *a*).$x_1(t)$, *b*).$x_2(t)$, *c*).$x_3(t)$, and *d*).$x_4(t)$.

$$A_8 = \begin{bmatrix} 0.0000 & 1.0000 & 0.0000 & 0.0000 \\ 3.6421 & 0.0018 & 0.0721 & 0.0002 \\ 0.0000 & 0.0000 & 0.0000 & 1.0000 \\ 2.4290 & -0.0305 & 2.9832 & -1.9 \times 10^{-5} \end{bmatrix},$$

$$A_9 = \begin{bmatrix} 0.0000 & 1.0000 & 0.0000 & 0.0000 \\ 6.2933 & -0.0009 & -0.2188 & -1.2 \times 10^{-5} \\ 0.0000 & 0.0000 & 0.0000 & 1.0000 \\ -7.4649 & 0.0024 & 3.2693 & 9.2 \times 10^{-6} \end{bmatrix},$$

$$B_{1,1} = \begin{bmatrix} 0 & 0 \\ 1 & -1 \\ 0 & 0 \\ -1 & 2 \end{bmatrix}, B_{1,2} = \begin{bmatrix} 0.0 & 0.0 \\ 0.5 & 0.0 \\ 0.0 & 0.0 \\ 0.0 & 1 \end{bmatrix}, B_{1,3} = 1 \begin{bmatrix} 0 & 0 \\ 1 & 1 \\ 0 & 0 \\ 1 & 2 \end{bmatrix},$$

$$B_{1,4} = \begin{bmatrix} 0 & 0 \\ 0.5 & 0 \\ 0 & 0 \\ 0 & 1 \end{bmatrix}, B_{1,5} = \begin{bmatrix} 0 & 0 \\ 1 & -1 \\ 0 & 0 \\ -1 & 2 \end{bmatrix}, B_{1,6} = \begin{bmatrix} 0 & 0 \\ 0.5 & 0 \\ 0 & 1 \end{bmatrix},$$

$$B_{1,7} = \begin{bmatrix} 0 & 0 \\ 1 & 1 \\ 0 & 0 \\ 1 & 2 \end{bmatrix}, B_{1,8} = \begin{bmatrix} 0 & 0 \\ 0.5 & 0 \\ 0 & 0 \\ 0 & 1 \end{bmatrix}, B_{1,9} = \begin{bmatrix} 0 & 0 \\ 1 & -1 \\ 0 & 0 \\ -1 & 2 \end{bmatrix},$$

$$C_i = \begin{bmatrix} 1 & 0 & 1 & 0 \end{bmatrix}, B_{2,i} = B_{1,i}, for\ i = 1, \ldots, 9.$$

Consider the nonlinear sliding coefficients as $k_1 = 10$, $k_2 = 20$; the initial state condition as $x(0) = \begin{bmatrix} -1 & 0 & 1 & 0 \end{bmatrix}^T$; the unmatched uncertainty as $d_{11}(x) = 0.01x_2(t)$, $d_{12}(x) = 0.01x_4(t)$; the matched uncertainty as $d_{21}(x) = 0.01x_1(t)$, $d_{22}(x) = 0.01x_3(t)$; the upper bounds uncertainty parameters as $\varepsilon = 10^{-8}$, $\eta_1 = 10^{-5}$, $\eta_2 = 0.1$, $\eta_3 = 0.1/k_1$; and the external disturbance as follows

$$w(t) = 0.005\cos(8\pi t) B_{2,i} \begin{bmatrix} 1 & 1 \end{bmatrix}^T$$

The desired transient time purpose is to assign the poles of each local linear subsystem into the region with $\alpha = 0.75$. Then, solving the GEVP optimization problem (58), we obtain the H_2 performance index from the external disturbance vector to the H_2 output vector as $\gamma = 3.5117$. The

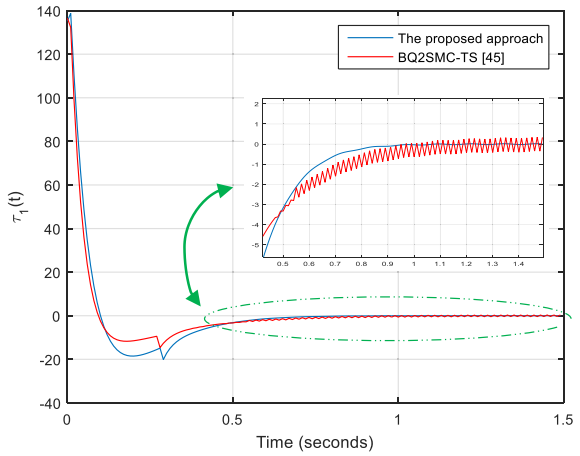

FIGURE 3. The control input signal $\tau_1(t)$.

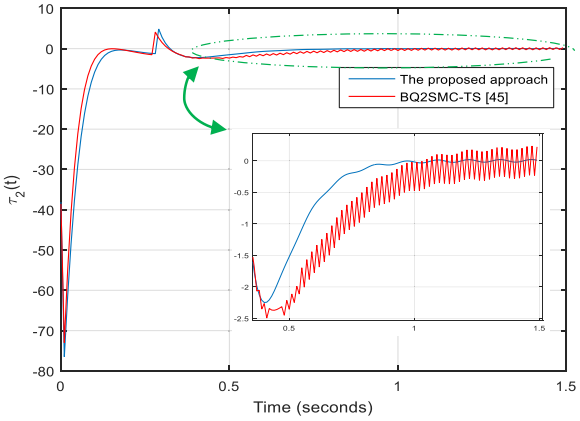

FIGURE 4. The control input signal $\tau_2(t)$.

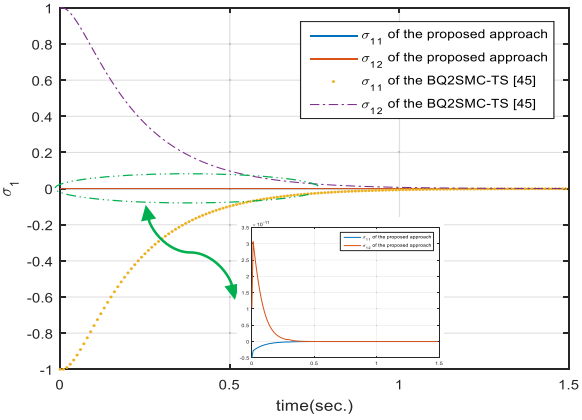

FIGURE 5. The evolution of the sliding surface $\sigma_1(t)$.

optimal sliding gains via GEVP optimization (61) is obtained as

$$S_1 = 10^{-13} \times \begin{bmatrix} 0.2070 & -0.1370 \\ -0.1598 & 0.3211 \end{bmatrix},$$

$$S_2 = 10^{-12} \times \begin{bmatrix} 0.3657 & -0.3869 \\ -0.7738 & 0.8473 \end{bmatrix},$$

$$S_3 = 10^{-11} \times \begin{bmatrix} 0.0076 & -0.0034 \\ -0.3480 & 0.3486 \end{bmatrix},$$

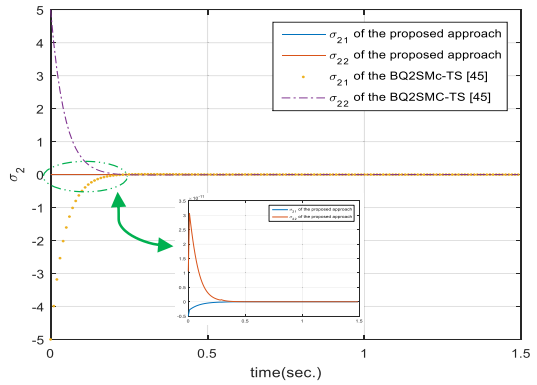

FIGURE 6. The evolution of the sliding surface σ_2(t).

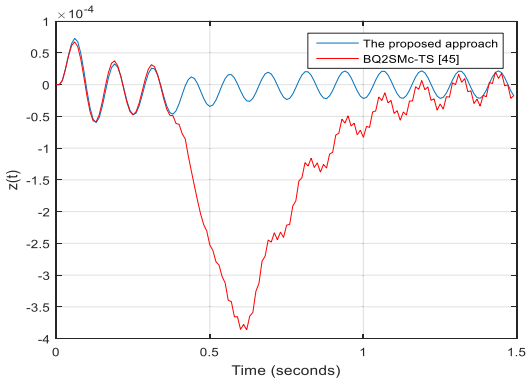

FIGURE 7. The trajectory of z (t).

$$S_4 = 10^{-12} \times \begin{bmatrix} 0.1918 & -0.2066 \\ -0.4132 & 0.4742 \end{bmatrix}$$

To compare the proposed approach efficacy with the similar works, a backstepping quasi-continues higher-order sliding mode controller (BQSMC_TS) for a TSFM [45] is studied under the same control signal effort. The illustrative comparison simulations are brought in Figs. 2-7.

VI. CONCLUSION

In this paper, for the strict-feedback form of the nonlinear systems represented by the TSFM, a new robust control scheme was developed based on BSMC. The proposed BSMC tries to design a novel multi-objective multi-sliding surfaces robust control against the uncertainties and the external disturbances. To do this, in the first step, a BSMC is developed to be optimized for the TSFM of the nonlinear system. Next, using a convex optimization approach, a state feedback gain is obtained for each fuzzy rule consequence subsystem while the H_2-norm constraints and also the α-stability constraint are satisfied. Then, the sliding surface gain is derived by solving the convex optimization problem associated with the state feedback obtained from the previous step. The proposed approach provides major advantages including: (i) the matched and the unmatched uncertainty can be manipulated concurrently; (ii) the adaptive laws were derived to estimate the unknown bounds of the uncertainties; (iii) the amplitude of the control efforts were constrained by the BSMC; (iv) another object, i.e. α-stability, was incorporated during the design SMC to improve the transient response indices; (v) sliding mode controller was computed by numerical methods.

The future works of this study may be directed to evolutionary algorithms for optimization, using more advanced and higher-order SMC approaches, or dynamic surface control-BSMC method to enhance the robustness and address stability issues. Moreover, relaxations in LMI design conditions may be noted.

REFERENCES

[1] K. Tanaka and H. O. Wang, *Fuzzy Control Systems Design and Analysis: A Linear Matrix Inequality Approach*. Hoboken, NJ, USA: Wiley, 2004.

[2] K. Ali, A. Mehmood, and J. Iqbal, "Fault-tolerant scheme for robotic manipulator-nonlinear robust back-stepping control with friction compensation," *PLoS ONE*, vol. 16, no. 8, 2021, Art. no. e0256491.

[3] L.-C. Guo, J. Ni, J.-B. Liu, X.-K. Fang, Q.-H. Meng, and Y.-D. Peng, "Backstepping output feedback control for the stochastic nonlinear system based on variable function constraints with the subsea intelligent electroexecution robot system," *Complexity*, vol. 2021, pp. 1–15, May 2021.

[4] F. Alyoussef and I. Kaya, "A review on nonlinear control approaches: Sliding mode control, back-stepping control and feedback linearization control," in *Proc. Int. Eng. Natural Sci. Conf. (IENSC)*, 2019, pp. 608–619.

[5] Q. Ye, C. Liu, and J. Sun, "A backstepping-based guidance law for an exoatmospheric missile with impact angle constraint," *IEEE Trans. Aerosp. Electron. Syst.*, vol. 55, no. 2, pp. 547–561, Apr. 2019.

[6] F.-J. Lin, S.-G. Chen, and C.-W. Hsu, "Intelligent backstepping control using recurrent feature selection fuzzy neural network for synchronous reluctance motor position servo drive system," *IEEE Trans. Fuzzy Syst.*, vol. 27, no. 3, pp. 413–427, Mar. 2019.

[7] R. S. Butt, I. Ahmad, R. Iftikhar, and M. Arsalan, "Integral backstepping and synergetic control for tracking of infected cells during early antiretroviral therapy," *IEEE Access*, vol. 7, pp. 69447–69455, 2019.

[8] M. S. Khan, I. Ahmad, and F. Z. U. Abideen, "Output voltage regulation of FC-UC based hybrid electric vehicle using integral backstepping control," *IEEE Access*, vol. 7, pp. 65693–65702, 2019.

[9] W. M. Haddad and V. Chellaboina, *Nonlinear Dynamical Systems and Control*. Princeton, NJ, USA: Princeton Univ. Press, 2011.

[10] X. Zhao, X. Wang, S. Zhang, and G. Zong, "Adaptive neural backstepping control design for a class of nonsmooth nonlinear systems," *IEEE Trans. Syst., Man, Cybern., Syst.*, vol. 49, no. 9, pp. 1820–1831, Sep. 2019.

[11] H. Ramirez-Rodriguez, V. Parra-Vega, A. Sanchez-Orta, and O. Garcia-Salazar, "Robust backstepping control based on integral sliding modes for tracking of quadrotors," *J. Intell. Robot. Syst.*, vol. 73, no. 4, pp. 51–66, 2014.

[12] Y. Wang and H. Wu, "Adaptive robust backstepping control for a class of uncertain dynamical systems using neural networks," *Nonlinear Dyn.*, vol. 81, no. 4, pp. 1597–1610, 2015.

[13] Y. Wang, L. Xu, and H. Wu, "Adaptive robust backstepping output tracking control for a class of uncertain nonlinear systems using neural network," *J. Dyn. Syst., Meas., Control*, vol. 140, no. 7, Jul. 2018, Art. no. 071014.

[14] A. Humaidi, M. Hameed, and A. Hameed, "Design of block-backstepping controller to ball and arc system based on zero dynamic theory," *J. Eng. Sci. Technol.*, vol. 13, no. 7, pp. 2084–2105, 2018.

[15] S. Rudra, R. K. Barai, and M. Maitra, "Nonlinear state feedback controller design for underactuated mechanical system: A modified block backstepping approach," *ISA Trans.*, vol. 53, no. 2, pp. 317–326, Mar. 2014.

[16] L. Ye, B. Tian, H. Liu, Q. Zong, B. Liang, and B. Yuan, "Anti-windup robust backstepping control for an underactuated reusable launch vehicle," *IEEE Trans. Syst., Man, Cybern., Syst.*, early access, Sep. 17, 2020, doi: 10.1109/TSMC.2020.3020365.

[17] X. Bu, X. Wu, R. Zhang, Z. Ma, and J. Huang, "Tracking differentiator design for the robust backstepping control of a flexible air-breathing hypersonic vehicle," *J. Franklin Inst.*, vol. 352, no. 4, pp. 1739–1765, Apr. 2015.

[18] L. Sonneveldt, Q. P. Chu, and J. A. Mulder, "Nonlinear flight control design using constrained adaptive backstepping," *J. Guid., Control, Dyn.*, vol. 30, no. 2, pp. 322–336, 2007.

[19] T. Jiang, D. Lin, and T. Song, "Finite-time backstepping control for quadrotors with disturbances and input constraints," *IEEE Access*, vol. 6, pp. 62037–62049, 2018.
[20] R. Liu and S. Li, "Optimal integral sliding mode control scheme based on pseudospectral method for robotic manipulators," *Int. J. Control*, vol. 87, no. 6, pp. 1131–1140, Jun. 2014.
[21] M. Vijay and D. Jena, "Backstepping terminal sliding mode control of robot manipulator using radial basis functional neural networks," *Comput. Electr. Eng.*, vol. 67, pp. 690–707, Apr. 2018.
[22] M. Khamar and M. Edrisi, "Designing a backstepping sliding mode controller for an assistant human knee exoskeleton based on nonlinear disturbance observer," *Mechatronics*, vol. 54, pp. 121–132, Oct. 2018.
[23] K. R. Muske, H. Ashrafiuon, S. Nersesov, and M. Nikkhah, "Optimal sliding mode cascade control for stabilization of underactuated nonlinear systems," *J. Dyn. Syst., Meas., Control*, vol. 134, no. 2, pp. 1–11, Mar. 2012.
[24] A. Ghasemian and A. Taheri, "Constrained near-time-optimal sliding-mode control of boost converters based on switched affine model analysis," *IEEE Trans. Ind. Electron.*, vol. 65, no. 1, pp. 887–897, Jan. 2018.
[25] J. Fang, S.-H. Tsai, J.-J. Yan, P. Chen, and S.-M. Guo, "Realization of DC–DC buck converter based on hybrid H_2 model following control," *IEEE Trans. Ind. Electron.*, vol. 69, no. 2, pp. 1782–1790, Feb. 2022.
[26] C. Liu, B. Jiang, R. J. Patton, and K. Zhang, "Decentralized output sliding-mode fault-tolerant control for heterogeneous multiagent systems," *IEEE Trans. Cybern.*, vol. 50, no. 12, pp. 4934–4945, Dec. 2020.
[27] Y. Zhang and Z. Shi, "Sliding mode control for uncertain T-S fuzzy singular biological economic system," *IEEE Access*, vol. 7, pp. 14387–14395, 2019.
[28] B. Tian, J. Cui, H. Lu, and Q. Zong, "Reentry attitude control for RLV based on adaptive event-triggered sliding mode," *IEEE Access*, vol. 7, pp. 68429–68435, 2019.
[29] G. Gao, M. Ye, and M. Zhang, "Synchronous robust sliding mode control of a parallel robot for automobile electro-coating conveying," *IEEE Access*, vol. 7, pp. 85838–85847, 2019.
[30] Y. Yu, H.-K. Lam, and K. Y. Chan, "T–S fuzzy-model-based output feedback tracking control with control input saturation," *IEEE Trans. Fuzzy Syst.*, vol. 26, no. 6, pp. 3514–3523, Dec. 2018.
[31] J. Hu, H. Zhang, X. Yu, H. Liu, and D. Chen, "Design of sliding-mode-based control for nonlinear systems with mixed-delays and packet losses under uncertain missing probability," *IEEE Trans. Syst., Man, Cybern., Syst.*, vol. 51, no. 5, pp. 3217–3228, May 2021.
[32] A. J. Koshkouei and A. S. Zinober, "Adaptive backstepping control of nonlinear systems with unmatched uncertainty," in *Proc. 39th IEEE Conf. Decis. Control*, vol. 5, Dec. 2000, pp. 4765–4770.
[33] S. Arora, P. Balsara, and D. Bhatia, "Input–output linearization of a boost converter with mixed load (constant voltage load and constant power load)," *IEEE Trans. Power Electron.*, vol. 34, no. 1, pp. 815–825, Jan. 2019.
[34] H. Wang, N. Li, Y. Wang, and B. Su, "Backstepping sliding mode trajectory tracking via extended state observer for quadrotors with wind disturbance," *Int. J. Control, Automat. Syst.*, vol. 19, no. 10, pp. 3273–3284, 2021.
[35] F. Chen, R. Jiang, K. Zhang, B. Jiang, and G. Tao, "Robust backstepping sliding-mode control and observer-based fault estimation for a quadrotor UAV," *IEEE Trans. Ind. Electron.*, vol. 63, no. 8, pp. 5044–5056, Aug. 2016.
[36] A. Argha, L. Li, and S. W. Su, "$\mathcal{H}_2$-based optimal sparse sliding mode control for networked control systems," *Int. J. Robust Nonlinear Control*, vol. 28, no. 1, pp. 16–30, 2018.
[37] Y. Aydin and I. Genc, "H_2 optimal control design with regional pole placement in power systems," *Impulse*, vol. 10, no. 10, p. 5, May 2007.
[38] M. Farsangi, Y. Song, and M. Tan, "Multi-objective design of damping controllers of FACTS devices via mixed H_2/H_∞ with regional pole placement," *Int. J. Elect. Power Energy Syst.*, vol. 25, no. 5, pp. 339–346, 2003.
[39] R. Zhang, L. Dong, and C. Sun, "Adaptive nonsingular terminal sliding mode control design for near space hypersonic vehicles," *IEEE/CAA J. Automatica Sinica*, vol. 1, no. 2, pp. 155–161, Apr. 2014.
[40] G. Xingquan and G. Shuang, "LMI-based H_2 control for T-S fuzzy system with hard constraints," *Int. J. Control Autom.*, vol. 8, no. 3, pp. 21–30, Mar. 2015.
[41] P. Apkarian, H. D. Tuan, and J. Bernussou, "Continuous-time analysis, eigenstructure assignment, and H_2 synthesis with enhanced linear matrix inequalities (LMI) characterizations," *IEEE Trans. Autom. Control*, vol. 46, no. 12, pp. 1941–1946, Dec. 2001.
[42] J. S. R. Jang, C. T. Sun, and E. Mizutani, "Neuro-fuzzy and soft Computing—A computational approach to learning and machine intelligence [book review]," *IEEE Trans. Autom. Control*, vol. 42, no. 10, pp. 1482–1484, Oct. 1997.
[43] S. Haykin, *Neural Networks: A Comprehensive Foundation*. Upper Saddle River, NJ, USA: Prentice-Hall, 1994.
[44] C.-S. Tseng, B.-S. Chen, and H.-J. Uang, "Fuzzy tracking control design for nonlinear dynamic systems via T-S fuzzy model," *IEEE Trans. Fuzzy Syst.*, vol. 9, no. 3, pp. 381–392, Jun. 2001.
[45] M. Van, H.-J. Kang, and K.-S. Shin, "Backstepping quasi-continuous high-order sliding mode control for a Takagi–Sugeno fuzzy system with an application for a two-link robot control," *Proc. Inst. Mech. Eng., C, J. Mech. Eng. Sci.*, vol. 228, no. 9, pp. 1488–1500, Jun. 2014.

FARZAD SOLTANIAN received the B.S. degree in electrical engineering from Shahid Rajaei Teacher Training University, Tehran, Iran, and the M.S. degree in electrical engineering from the Sahand University of Technology, Tabriz, Iran, in 2008 and 2011, respectively. He is currently pursuing the Ph.D. degree in electrical engineering with the Shiraz University of Technology, Shiraz, Iran.

His research interests include the Takagi-Sugeno fuzzy-based nonlinear control, robust control design, robotic, and fault-tolerant control design.

MOKHTAR SHASADEGHI is currently an Associate Professor with the Shiraz University of Technology, Shiraz, Iran. His research interests include fuzzy control, linear matrix inequalities, and optimization.

SALEH MOBAYEN (Senior Member, IEEE) received the B.Sc. and M.Sc. degrees in control engineering from the University of Tabriz, Tabriz, Iran, in 2007 and 2009, respectively, and the Ph.D. degree in control engineering from Tarbiat Modares University, Tehran, Iran, in January 2013. From February 2013 to December 2018, he was an Assistant Professor and a Faculty Member with the Department of Electrical Engineering, University of Zanjan, Zanjan, Iran, where he has been an Associate Professor of control engineering with the Department of Electrical Engineering, since December 2018. Currently, he collaborates with the National Yunlin University of Science and Technology as an Associate Professor with the Future Technology Research Center. His research interests include control theory, sliding mode control, robust tracking, non-holonomic robots, and chaotic systems.

AFEF FEKIH (Senior Member, IEEE) received the B.S., M.S., and Ph.D. degrees in electrical engineering from the National Engineering School of Tunis, Tunisia, in 1995, 1998, and 2002, respectively. She is currently a Full Professor with the Department of Electrical and Computer Engineering and also the Chevron/BORSF Professor of engineering with the University of Louisiana, Lafayette. Her research interests include control theory and applications, including nonlinear and robust control, optimal control, and fault-tolerant control with applications to power systems, wind turbines, unmanned vehicles, and automotive engines. She is a member of the IEEE Control Systems Society and the IEEE Women in Control Society.